

Original Research Article

**Design of Novel Drugs (P3TZ, H2P3TZ, M2P3TZ, H4P3TZ and M4P3TZ)
Based on Zonisamide for Autism Treatment by Binding to Potassium Voltage-
gated Channel Subfamily D Member 2 (Kv4.2)**

Mehdi Nabati* and Vida Bodaghi-Namileh

*Synthesis and Molecular Simulation Laboratory, Chemistry Department, Pars Isotope Company, P.O.
Box: 1437663181, Tehran, Iran*

* Corresponding author Tel number: +982188337023, Fax number: +982188337024

*E-mail: mnabati@ymail.com

ABSTRACT

The present research article relates to the discovery of the novel drugs based on Zonisamide to treatment of autism disease. In first step, the electronic properties, reactivity and stability of the said compound are discussed. To attain these properties, the said molecular structure is optimized using B3LYP/6-311++G(d,p) level of theory at room temperature. The frontier molecular orbitals (FMOs) energies are used to calculate the global reactivity indices. Based on these indices, Zonisamide is a high stable compound and has low reactivity. In the next step, the optimized molecular structure of Zonisamide is docked into the potassium voltage-gated channel subfamily D member 2 (Kv4.2) and ligand-receptor interactions are analyzed. After that, the novel molecular structures based on Zonisamide backbone are designed and optimized. Designing the novel drugs are done using changes the backbone of Zonisamide and various functional groups. The interactions of the optimized molecular structures with the said potassium

channel are analyzed using docking study. Based on these studies, ten molecules showed better ligand-receptor binding than Zonisamide. Finally, the physicochemical properties of the title compounds are analyzed. The compounds P3TZ, H2P3TZ, M2P3TZ, H4P3TZ and M4P3TZ are our novel drugs to treatment of autism disease based on the molecular docking and physicochemical properties.

Keywords: *Autism; Drug design; Molecular docking; Molecular simulation; potassium channel; Zonisamide.*

Introduction

Autism spectrum disorders (ASDs) are complex and prevalent neurodevelopmental disorders predominantly diagnosed through observation of a wide variety of atypical behavior, expressed by impairments in socialization, communication, thinking, interests, activities and cognitive skills as well as restricted and repetitive behavior. Autism is considered a heterogeneous condition with both medical and psychiatric comorbidities [1, 2]. Medical comorbidities include gastrointestinal disorders, neuro-inflammation, immune system disorders, vitamin deficiencies, sleep disorders and epilepsy while psychiatric comorbidities include attention-deficit hyperactivity disorder, social anxiety disorder, depression, bipolar disorder and intellectual disability [3]. The risk of premature mortality in ASD patients has been observed to be noticeably higher in comparison with the general population [5-8]. Moreover, this condition imposes a financial burden on families, society and health systems [9, 10]. Several interventions and treatments have been considered for the management of ASD, mostly focusing on ameliorating comorbidities and enhancing the quality of life in patient afflicted with this disorder. The precise mechanism of ASD pathogenesis is not yet fully understood and has been associated with both genetic and non-genetic factors [11-16]. Recent genetic analyses have uncovered important evidence pertaining to the role of potassium channels in etiology of ASD. The A-type voltage-gated potassium channel Kv4.2 is encoded by KCND2. Mutations of the Kv4.2 channel gene have been associated with ASD onset [17]. Furthermore, Kv4.2 mRNA

binds to fragile X mental retardation protein (FMRP) also known as synaptic functional regulator FMR1. FMRP is a protein which binds to hundreds of mRNAs, regulating their translation in postsynaptic neurons. The loss of FMRP as a consequent of mutations in FMR1 gene, leads to fragile X syndrome (FXS), which is the leading genetic cause of autism in about 5 percent of ASD patients. Therefore, induction of Kv4.2 channel expression has been implied to play an important role in etiology of ASD [18, 19]. In this regard, it was hypothesized that potassium channel blockers specific for Kv4.2 subunit could be utilized to manage ASD. Zonisamide (ZNS) is a drug used mostly in treatment of epilepsy and management of both focal and generalized seizures [20-22]. Recently, the use of this drug in other neurological disorders such as Parkinson has been evaluated [23-25]. Zonisamide exerts its effects through multiple routes. The most predominant mechanism of action for Zonisamide is the blockage of voltage-dependent sodium and T-type calcium channels. Furthermore, the drug was also reported to effectively block A-type potassium channels in hippocampal cells [26, 27]. Based on our survey through previous studies, it was surmised that the drugs used for autism generally consist NH_2 , OH , OCH_3 , COOH functional groups as well as nitrogen containing rings such as pyridine. In this respect, the present study focused on the design of an analog of Zonisamide with the best structural interactions with potassium channel Kv4.2. For this purpose, the aforementioned functional groups were substituted in the compound's structure and the efficiency and affinity towards Kv4.2 was evaluated using molecular docking methods and computational chemistry. Furthermore, the pharmacokinetic and biological behavior of each individual compound was assessed by SwissADME web tool.

Computational methods

Identification of novel medicines is done in the process of drug discovery. This field of medicine and pharmacology contains a complicated relationship among the different sciences including chemistry, pharmacology and biology. A theoretical drug discovery process contains three steps: quantum mechanical study of the designed molecular structures, their binding to the receptors and analyzing their physicochemical properties [28-32]. Here, the structural and electronic properties of Zonisamide and the designed chemical compounds are studied using density functional theory (DFT) computational method. Firstly, All molecular structures are optimized

using B3LYP/6-311++G(d,p) level of theory in isolated form at room temperature. The QM computations are done by Gaussian 03 software. Then, their stability and reactivity properties are discussed by frontier molecular orbitals (FMOs) calculations. Finally, all optimized molecular structures are docked into the potassium voltage-gated channel subfamily D member 2 (Kv4.2) and analyzed. The crystal structure of the said protein was taken from the PDB (<https://www.rcsb.org/>). The Molegro Virtual Docker (MVD) software is used to the molecular docking analyses. On the other hand, the physicochemical properties of the designed molecules are simulated using the online web tool www.swissadme.ca and discussed. The drug-likeness properties were analyzed using the FAF-Drugs4 server.

Results and discussion

Zonisamide structural and electronic properties study

The first step in drug discovery is finding the good computational method to simulation of the molecular structure of the designed novel drugs. Hence, we tested various quantum mechanical based computational methods on Zonisamide molecular structure (Figure 1). In each method, we compared the theoretical bond lengths of the said compound with the experimental data. In B3LYP/6-311++G(d,p) computational method, the dependence is shown by the equation $y=0.9964x-0.0084$ (Figure 2). The higher correlation coefficient ($R^2=0.9137$) for this equation shows a great convergence. So, the B3LYP/6-311++G(d,p) basis set of theory is a good method to compute the electronic properties of the title compound. The optimized molecular structure indicates that the benzo[d]isoxazole backbone is planar and obeys from Huckel rule ($4n+2 e$). So, it is an aromatic **molecular structure**.

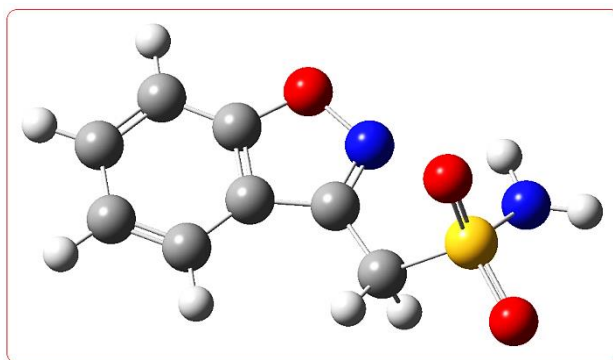
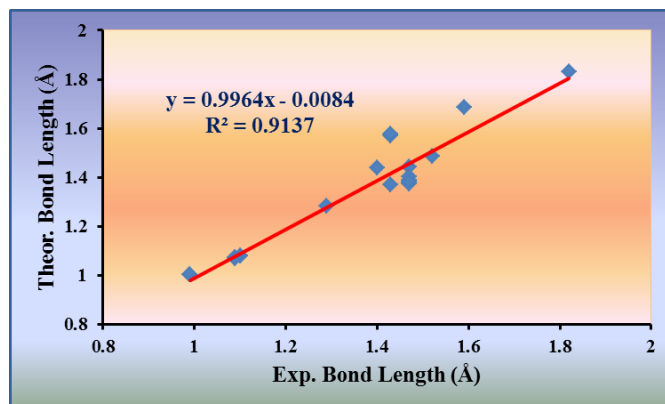


Figure 1. The optimized molecular structure of Zonisamide**Figure 2.** The experimental and theoretical bond lengths relationship of Zonisamide

Stability and reactivity are two important parameters for each chemical compound which should be a medicinal substance. These parameters can be discussed using frontier molecular orbitals (FMOs) theory. The frontier molecular orbitals are called to the highest occupied and lowest unoccupied molecular orbitals (HOMO and LUMO) [33-35]. The frontier molecular orbitals of Zonisamide are shown in Figure 3. We can see the lowest unoccupied molecular orbital is made by all atoms of the said compound. So, all atoms of the molecule can be interacted with electron rich agents. In contrast, only the atoms of the benzo[d]isoxazole ring are participated in making the highest occupied molecular orbital. This means the atoms of the benzo[d]isoxazole can be interacted with electron poor residues of the proteins. On the other hand, the molecular electrostatic potential (MEP) is a key parameter to describe the charge distribution on the molecular structure of a compound [36]. The negative, zero and positive potentials are shown by red, green and blue colors, respectively. The MEP graph of Zonisamide molecular structure indicates the benzo[d]isoxazole ring potential is zero. Only the SO_2NH_2 functional group shows negative charge potential. So, it can be predicted this molecule has low interactions with biomolecules. For good discussion about the stability and reactivity properties of the said compound, the global reactivity descriptors like energy gap (E_g), ionization potential (IP), electron affinity (EA), chemical hardness (η), chemical softness (S), electronegativity (χ), electronic chemical potential (μ) and electrophilicity index (ω) will be computed from the

energies of the frontier orbitals. These global reactivity indices are achieved by following formulas [37]:

$$E_g = E_{LUMO} - E_{HOMO}$$

$$IP = -E_{HOMO}$$

$$EA = -E_{LUMO}$$

$$\eta = \frac{(\varepsilon_{LUMO} - \varepsilon_{HOMO})}{2}$$

$$\chi = \frac{-(\varepsilon_{LUMO} + \varepsilon_{HOMO})}{2}$$

$$\mu = \frac{(\varepsilon_{LUMO} + \varepsilon_{HOMO})}{2}$$

$$\omega = \frac{\mu^2}{2\eta}$$

$$S = \frac{1}{\eta}$$

Table 1 has been listed the global reactivity indices and frontier molecular orbitals energies of the active substance Zonisamide. From the data of the Table 1, the energies of HOMO and LUMO are -9.88 eV and 1.76 eV, respectively. The low energy of the frontier molecular orbitals shows the stability of the said compound. The HOMO-LUMO energies gap is 11.64 eV. This high energy gap indicates that the electron transition may not happen from HOMO to LUMO. The density of states (DOS) graph shows that occupied molecular orbitals have more density than the virtual ones. On the other hand, it is predicted the molecule can hardly be participated in interactions with redox agents due to its high ionization potential amount. So, the molecule prefers to keep its neutral state. The high chemical hardness and low chemical softness indices explain the low reactivity of the title compound with biomolecules.

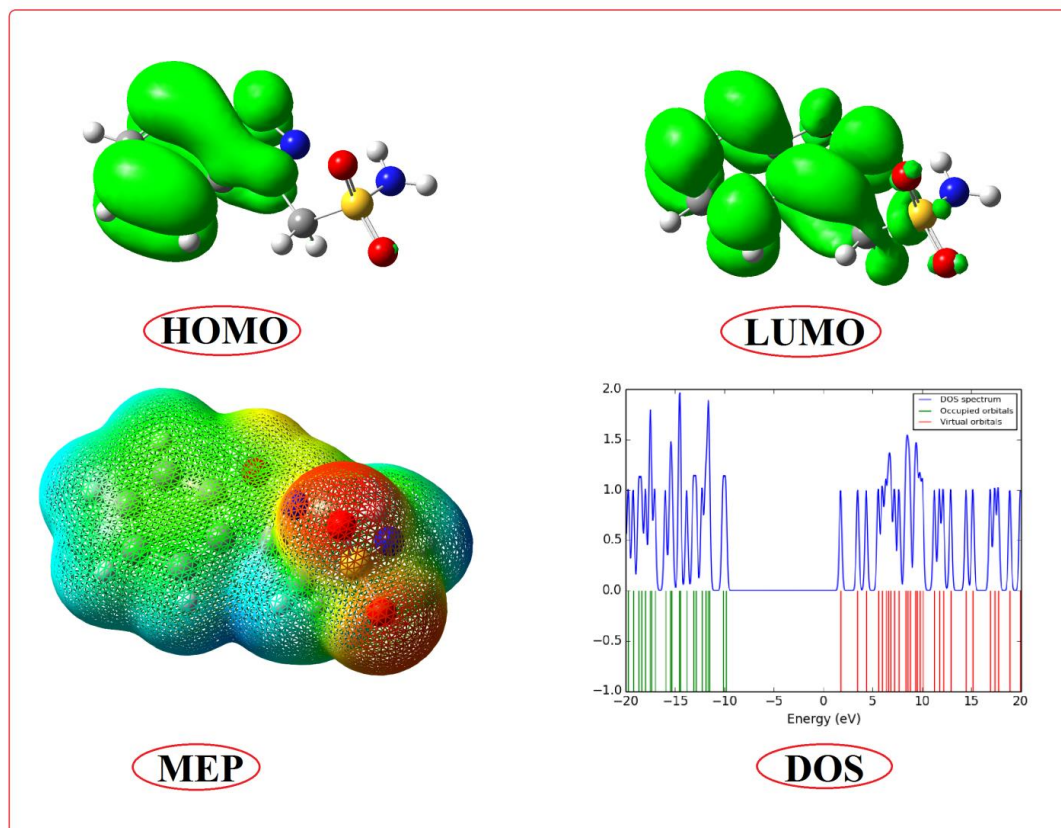


Figure 3. The FMOs, MEP and DOS graphs of Zonisamide

Table 1. Global reactivity indices of Zonisamide

Parameter	Energy value (eV)
HOMO	-9.88
LUMO	1.76
Ionization Potential (IP)	9.88
Electron Affinity (EA)	-1.76
Energy Gap (Eg)	11.64
Electronegativity (χ)	4.06
Chemical Potential (μ)	-4.06
Chemical Hardness (η)	5.82
Chemical Softness (S)	0.172
Electrophilicity index (ω)	1.416

Molecular docking analysis of Zonisamide binding to the potassium voltage-gated channel subfamily D member 2 (Kv4.2)

Molecular docking is a key tool in structural molecular biology and computer assisted drug design [38]. This approach is used to analysis of the binding modes of a medicinal compound with a biomolecule like receptor [39, 40]. Here, the optimized molecular structure of Zonisamide is docked into the potassium voltage-gated channel subfamily D member 2 (Kv4.2) and its binding to the residues are discussed (Figure 4). Our computations show the energy of the Zonisamide interaction with the receptor is -81.8229 (MolDock score). Binding the drug to the receptor is carried out using steric interactions (score = -65.072) and hydrogen bond interactions (score = -0.09). On the other hand, the title ligand is interacted with two water molecules by score -16.47. The steric interactions of the said compound are done with residues Phe 84, Phe 85, His 77, Asp 86, Tyr 76, Phe 74, Phe 75, Phe 121 and Arg 87. In contrast, only the residue Asp 86 from the receptor is participated in making the hydrogen bond with Zonisamide. In overall, the residues Phe 75, Asp 86, Phe 84 and Phe 74 play main role in making the ligand-receptor complex.

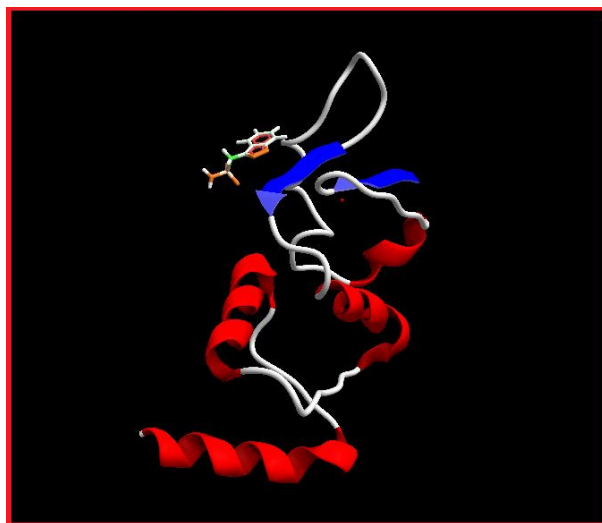
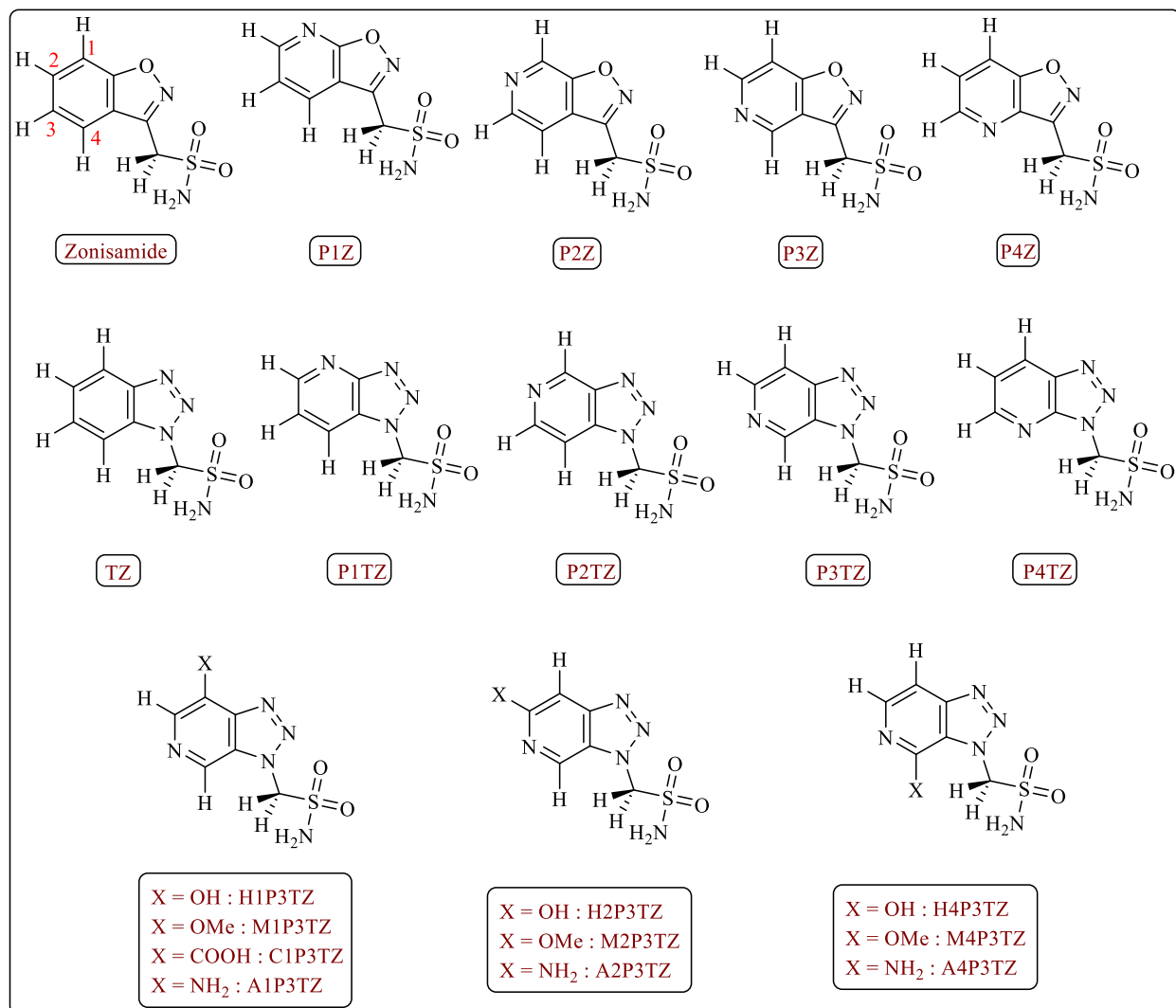


Figure 4. Ligand Zonisamide embedded in the active site of the potassium voltage-gated channel Kv4.2

Docking analysis of the novel designed molecular structures

As described above, Zonisamide can make complex with the potassium voltage-gated channel Kv4.2. To increase the binding power of drug to the receptor, the novel molecular structures are designed by changing the Zonisamide backbone and adding various substituents. The molecular structures of Zonisamide and designed compounds are indicated in Scheme 1.



Scheme 1. The designed molecular structures based on Zonisamide

Our studies showed the autism treatment drugs have the rings containing nitrogen element in their molecular structures. Hence, we designed new molecular structures based on Zonisamide

that they have pyridine and or triazole rings in their backbone. The designed molecular structures are P1Z, P2Z, P3Z, P4Z, TZ, P1TZ, P2TZ, P3TZ and P4TZ. Firstly, all molecular structures were optimized at B3LYP/6-311++G(d,p) level of theory. Then, the optimized molecular structures are docked into the potassium voltage-gated channel Kv4.2. The docking analysis data of the complexes of the designed molecular structures and the protein is listed in Table 2. As can be seen from the data of the Table 2, only the molecules TZ, P1TZ, P2TZ, P3TZ and P4TZ showed the better ligand-protein binding than the Zonisamide-receptor complex. Also, the molecular structure P3TZ showed the most powerful interaction with the receptor.

Table 2. Docking analysis data of the designed molecular structures based on changing the Zonisamide backbone

Compound	Moldock Score
Zonisamide	-81.8229
P1Z	-78.8104
P2Z	-81.5662
P3Z	-81.3524
P4Z	-80.3933
TZ	-85.7690
P1TZ	-82.8567
P2TZ	-83.7584
P3TZ	-86.0917
P4TZ	-85.4421

After identifying the best designed backbone (P3TZ), we tested various substituents (COOH, NH₂, OH and OMe) on this molecule. Similarly the previous section, all designed compounds were optimized and docked into the receptor. Table 3 has collected the docking analysis data of the complexes of the designed molecules with the receptor. As can be shown from the data, all molecules except M1P3TZ have good interaction with the receptor.

Table 3. The molecular structures-receptor docking analysis data

Compound	Moldock Score
P3TZ	-86.0917
H1P3TZ	-91.7934
M1P3TZ	-81.1090
A1P3TZ	-94.5526
C1P3TZ	-90.9534
H2P3TZ	-89.1873
M2P3TZ	-88.5182
A2P3TZ	-90.9899
H4P3TZ	-94.7925
M4P3TZ	-91.2820
A4P3TZ	-94.9668

Physicochemical descriptors and ADME parameters of the designed compounds

As mentioned above, the docking results indicated better receptor interactions in all of the investigated compounds compared with Zonisamide (with the exception of M1P3TZ). In addition, the prediction of physiochemical descriptors and ADME behavior of molecular compounds is considered a predominant factor in early stages of drug discovery. ADME parameter of the best ten compounds was predicted using SwissADME web tool. The results for computed analysis of these compounds are presented in Tables 4 and 5. The first section evaluates *physiochemical properties*, including molecular formula, molecular weight, the number of heavy atoms and aromatic heavy atoms, fraction csp³, the number of rotatable bond, H-bond receptors and H-bond donors, molar refractivity and TPSA (Topological Polar Surface Area). The next factor which greatly contributes to drug discovery and compound design is *lipophilicity*. Lipophilicity values not only impact solubility but also influence permeability

through biological membranes, potency, selectivity and toxicity. Lipophilicity is determined by measuring the partition coefficient between n-octanol and water ($\log PO/W$). ADME utilizes five predictive models regarding lipophilicity of the compounds (iLOGP, XLOGP, WLOGP, MLOGP and SILICOS-IT). The investigated molecules displayed almost similar lipophilicity profile with MLOGP values of -1.67 in P3TZ, -1.79 in A2P3TZ, H2P3TZ, A4P3TZ and H4P3TZ, -1.44 in M2P3TZ and M4P3TZ, -2.20 in A1P3TZ and H1P3TZ and finally -2.99 in C1P3TZ. *Water solubility* is one of the most important parameters influencing bioavailability of the drugs and achieving optimal drug concentration in systemic circulation. Predicting water solubility is especially important in oral pharmaceutical dosage forms and is the basic requirement for the drug's absorption from Gastrointestinal track (GIT). Water solubility of the compounds was determined using ESOL model, a topical method to evaluate $\log S$. In this respect, the compounds are placed into six categories: 1) Insoluble ($\log S < -10$), 2) Poorly soluble ($-10 < \log S < -6$), 3) Moderately soluble ($-6 < \log S < -4$), 4) Soluble ($-4 < \log S < -2$), 5) Very soluble ($-2 < \log S < 0$) and 6) Highly soluble ($\log S > 0$). As can be observed in Tables 4 and 5, all substitutions fall into very soluble category. Individual ADME behaviors of the molecules under investigation are evaluated in *pharmacokinetics* section which evaluates the compounds passive gastrointestinal (GI) absorption, Blood Brain Barrier (BBB) permeability, P-gp efflux, inhibition of Cytochrome P450 enzymes (CYP1A2, CYP2C19, CYP2C9, CYP2D6 and CYP3A4). GI absorption is presented as high and low values. Compounds P3TZ, H1P3TZ, H2P3TZ, H4P3TZ, M2P3TZ and M4P3TZ all displayed high GI absorptions while A1P3TZ, A2P3TZ, A4P3TZ and H1P3TZ showed low GI absorptions. Furthermore, none of the investigated structures are BBB permeant and P-gp efflux pump substrates. Cytochrome P450 superfamily of isoenzymes plays a major role in drug elimination through metabolic biotransformation, therefore, inhibition of these enzymes is of particular importance in pharmacokinetics-related drug-drug interactions and toxic or adverse effects due to the decreased clearance and accumulation of the drug or its metabolites. Neither of the mentioned compounds inhibits cytochrome P450 enzymes. Lipinski's rule of five and bioavailability score of the chosen compounds determines their *drug-likeness*. All 10 compounds abide Lipinski's rule ($MLOGP \leq 4.15$, relative MW ≤ 500 , N or O ≤ 10 , NH or OH ≤ 5). Bioavailability score is used to forecast the permeability and bioavailability properties of a compound in discovery setting. The values

are 0.55 in all investigated compounds with the exception of C1P3TZ which has a bioavailability score of 0.56.

Table 4. ADME properties of P3TZ, H1P3TZ, A1P3TZ, C1P3TZ and H2P3TZ

Compounds					
Physiochemical descriptors and ADME parameters	P3TZ	H1P3TZ	A1P3TZ	C1P3TZ	H2P3TZ
Formula	C ₆ H ₇ N ₅ O ₂	C ₆ H ₇ N ₅ O ₃	C ₆ H ₈ N ₆ O ₂	C ₇ H ₇ N ₅ O ₄	C ₆ H ₇ N ₅ O ₃
	S	S	S	S	S
MW (g/mol)	213.22	229.22	228.23	257.23	229.22
Num. Heavy Atoms	14	15	15	17	15
Num. Arom. Heavy Atoms	9	9	9	9	9
Fraction Csp³	0.17	0.17	0.17	0.14	0.17
Num. Rotatable bonds	2	2	2	3	2
Num. H-bond acceptors	6	7	6	8	7
Num. H-bond donors	1	2	2	2	2
Molar Refractivity	48.26	50.28	52.66	55.22	50.28
TPSA (Å²)	112.14	132.37	138.16	149.44	132.37
MLOGP	-1.67	-2.20	-2.20	-2.99	-1.79
Log S (ESOL)	-0.74	-0.58	-0.37	-0.56	-0.79
Class	Very Soluble	Very Soluble	Very Soluble	Very Soluble	Very Soluble
GI Absorption	High	High	Low	Low	High
BBB permeant	No	No	No	No	No
P-gp substrate	No	No	No	No	No

PYP450 inhibitor	No	No	No	No	No
Lipinski	Yes	Yes	Yes	Yes	Yes
Bioavailability Score	0.55	0.55	0.55	0.56	0.55

Table 5. ADME properties of M2P3TZ, A2P3TZ, H4P3TZ, M4P3TZ and A4P3TZ

Compounds					
Physiochemical descriptors and ADME parameters	M2P3TZ	A2P3TZ	H4P3TZ	M4P3TZ	A4P3TZ
Formula	C ₆ H ₉ N ₅ O ₃ S	C ₆ H ₈ N ₆ O ₂ S	C ₆ H ₇ N ₅ O ₃ S	C ₇ H ₉ N ₅ O 3S	C ₆ H ₈ N ₆ O 2S
MW (g/mol)	243.24	228.23	229.22	243.24	228.23
Num. Heavy Atoms	16	15	15	16	15
Num. Arom. Heavy Atoms	9	9	9	9	9
Fraction Csp³	0.29	0.17	0.17	0.29	0.17
Num. Rotatable bonds	3	2	2	3	2
Num. H-bond acceptors	7	6	7	7	6
Num. H-bond donors	1	2	2	1	2
Molar Refractivity	54.75	52.66	50.28	54.75	52.66
TPSA (Å²)	121.37	138.16	132.37	121.37	138.16
MLOGP	-1.44	-1.79	-1.79	-1.44	-1.79
Log S (ESOL)	-0.99	-0.58	-0.79	-0.99	-0.58
Class	Very Soluble	Very Soluble	Very Soluble	Very Soluble	Very Soluble
GI Absorption	High	Low	High	High	Low

BBB permeant	No	No	No	No	No
P-gp substrate	No	No	No	No	No
PYP450 inhibitor	No	No	No	No	No
Lipinski	Yes	Yes	Yes	Yes	Yes
Bioavailability Score	0.55	0.55	0.55	0.55	0.55

The structures went under further analysis using FAFdrugs4 web tool. The results are presented in Figures 5-10. Figure 5 is Physchem Filter Positioning which provides a radar plot, incorporating all assessed physiochemical descriptors. The compound's values (blue line) should fall within the drug-like filter area (pale blue and red). As observed in Figure 5, all compounds reside in the specified ranges.

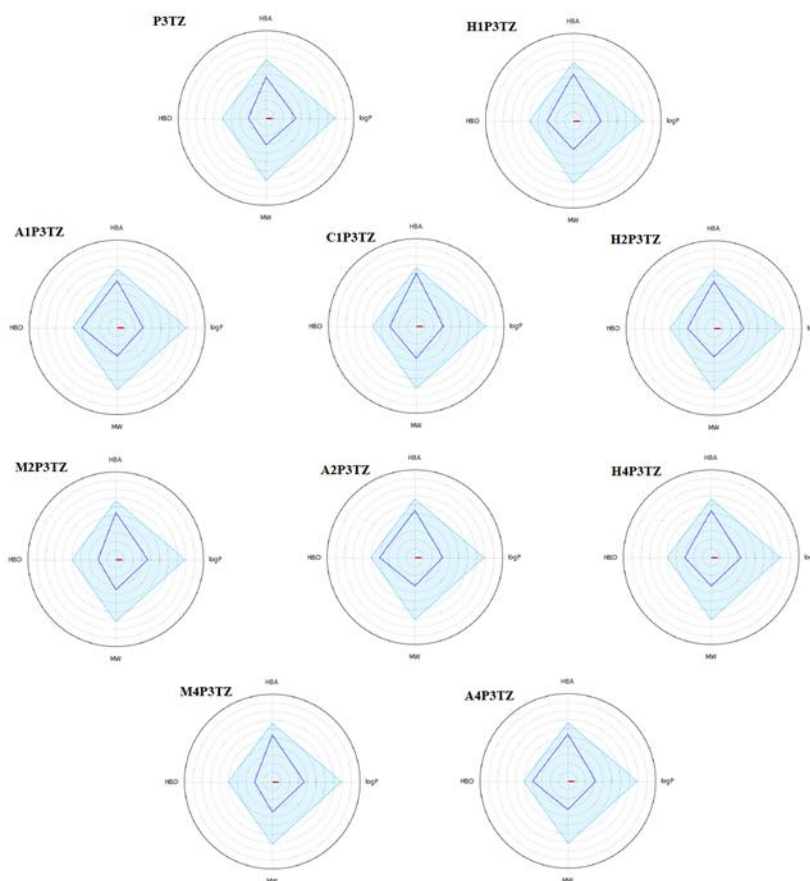


Figure 5. PhysChem Filter Positioning of P3TZ, H1P3TZ, A1P3TZ, C1P3TZ, H2P3TZ, M2P3TZ, A2P3TZ, H4P3TZ, M4P3TZ and A4P3TZ

Figure 6 visualizes Compound Complexity. It includes the number of system ring, stereo centers, rotatable and rigid bonds, the flexibility (ration between rotatable and rigid bonds), the carbon saturation (fsp3 ratio) and the maximum size of system rings. The values for all 10 compounds (blue line) fall within the oral library min and max ranges (determined by red and pink areas).

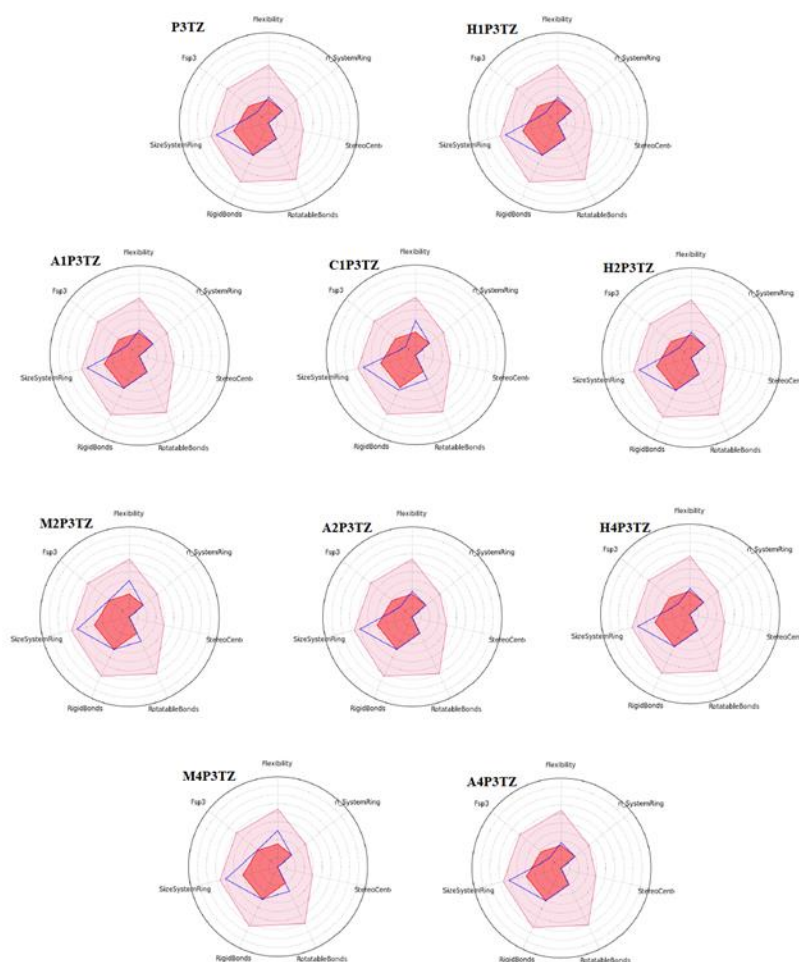


Figure 6. Compound Complexity of P3TZ, H1P3TZ, A1P3TZ, C1P3TZ, H2P3TZ, M2P3TZ, A2P3TZ, H4P3TZ, M4P3TZ and A4P3TZ

Figure 7 analyses Golden Triangle Rule which is a visualization tool used to optimize clearance and oral absorption of drug candidates. The compounds superimposed in the triangle are likely to

possess optimal permeability (low clearance) and a good metabolic stability. As presented in Figure 7, the compounds P3TZ, M3P3TZ, A2P3TZ, H4P3TZ and M4P3TZ all fall within, whereas H1P3TZ, C1P3TZ and A1P3TZ are located outside of the golden triangle. In addition, A2P3TZ and A4P3TZ are resided on the border.

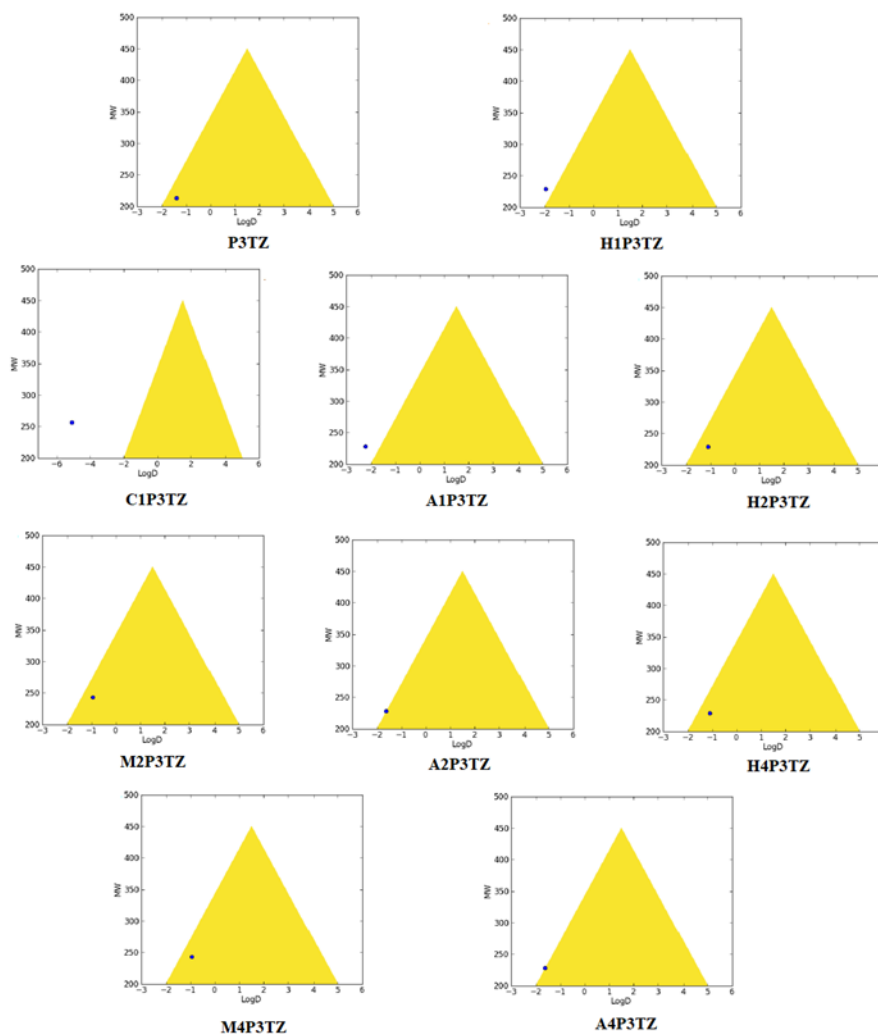


Figure 7. Golden Triangle Rule for P3TZ, H1P3TZ, A1P3TZ, C1P3TZ, H2P3TZ, M2P3TZ, A2P3TZ, H4P3TZ, M4P3TZ and A4P3TZ

Figure 8 represents Oral Property Space, which is obtained by applying the PCA (Principal Component Analysis) of the 15 main physico-chemical descriptors of the chosen compounds (red), compared with two oral libraries extracted from eDrugs (blue) and DrugBank (orange). All compounds are located within the specified range.

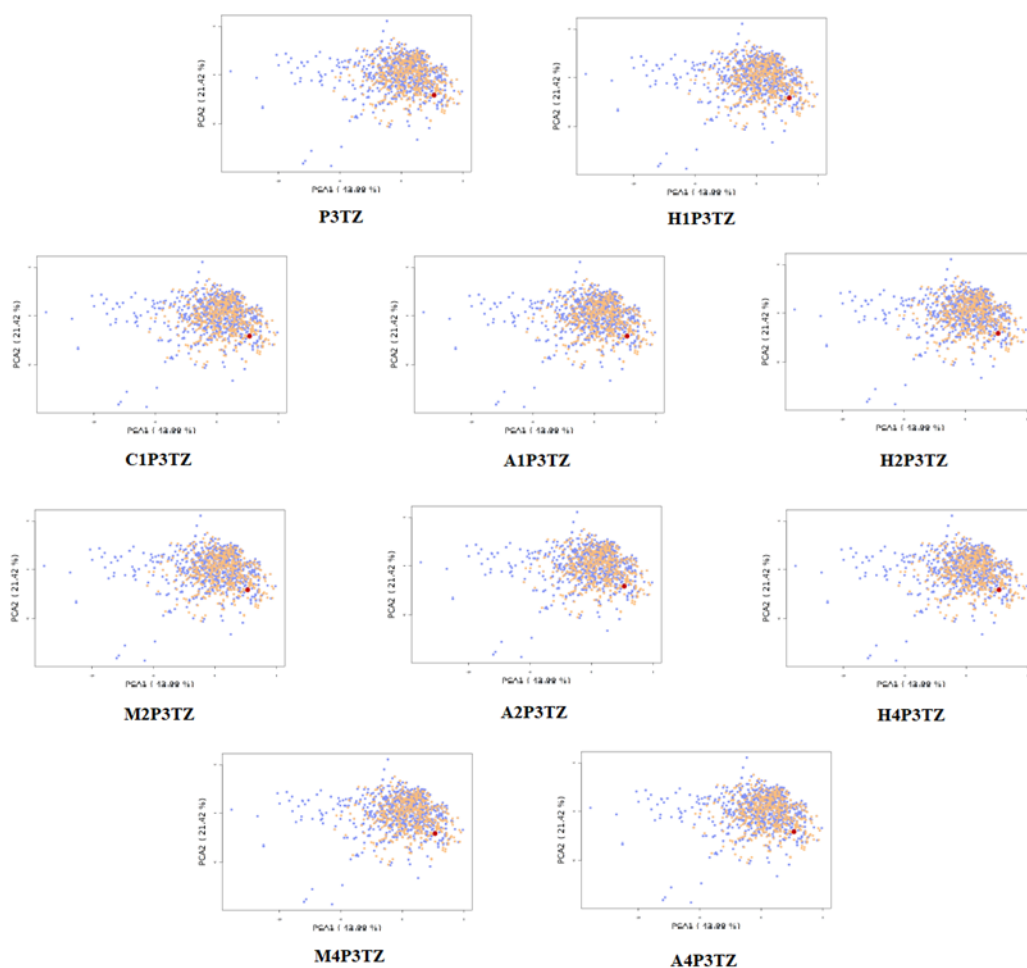


Figure 8. Oral Property Space of P3TZ, H1P3TZ, A1P3TZ, C1P3TZ, H2P3TZ, M2P3TZ, A2P3TZ, H4P3TZ, M4P3TZ and A4P3TZ

Oral Absorption Estimation is presented in Figure 9. The compounds values are materialized by the blue line, which should fall within the optimal green area (Rule of 5 and Verber rule area).

The white area is the extreme maximum zone and the red one is the extreme minimum zone.

These zones are determined by the following descriptors ranges: LOGP (-2 to 5), MW (150 to 500), tPSA (20 to 150), Rotatable Bonds (0 to 10), H-Bonds Acceptors (0 to 10) and Donors (0 to 5).

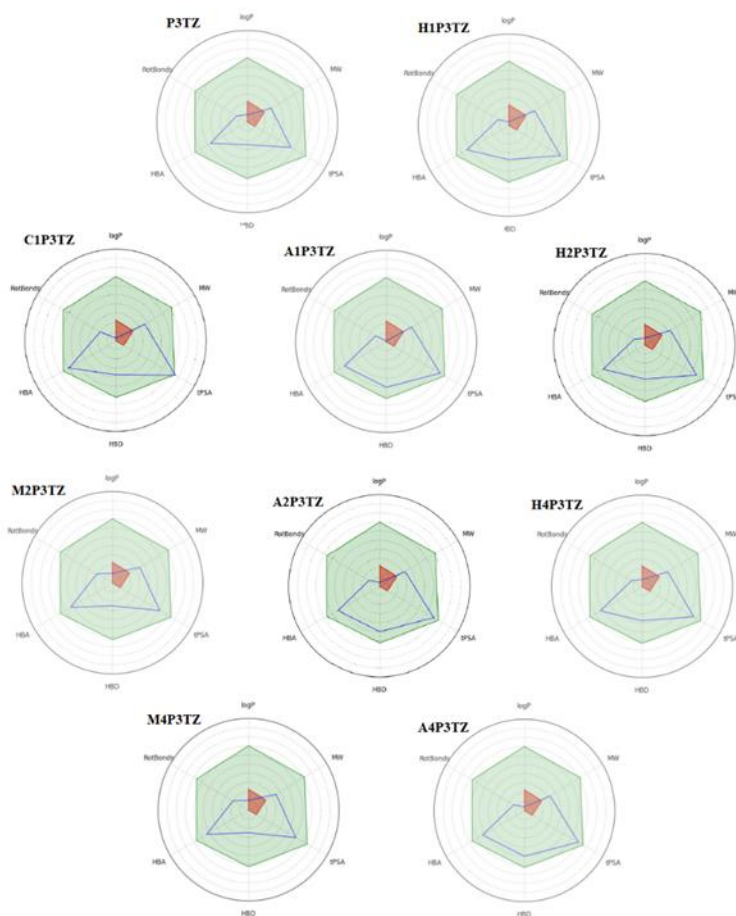


Figure 9. Oral Absorption Estimation of P3TZ, H1P3TZ, A1P3TZ, C1P3TZ, H2P3TZ, M2P3TZ, A2P3TZ, H4P3TZ, M4P3TZ and A4P3TZ

All 10 compounds are located within acceptable ranges. Lastly, *Pfizer 3/75 rule* is exhibited in Figure 10. Molecules located in red square are more likely to cause toxicity. The compounds under investigation are all placed in the green square predicting them to be non-toxic. Regarding the obtained data from physiochemical properties and pharmacokinetic behaviors of our best compounds and considering the oral route of administration, we decided to administer further filters in order to introduce candidates with the best properties. The investigated compounds mostly showed similar properties except for GI absorption and clearance (golden triangle rule). The 5 final compounds with both high GI absorption and optimal clearance are P3TZ, H2P3TZ, M2P3TZ, H4P3TZ and M4P3TZ.

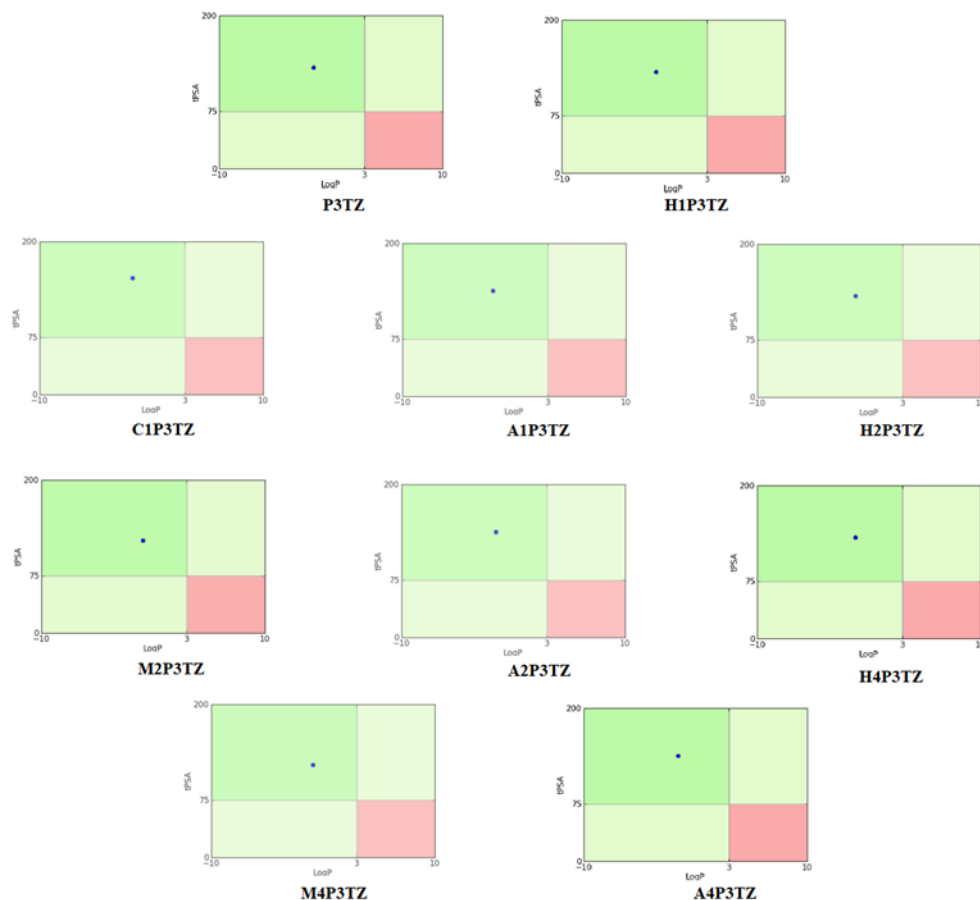


Figure 10. Pfizer 3/75 rule of P3TZ, H1P3TZ, A1P3TZ, C1P3TZ, H2P3TZ, M2P3TZ, A2P3TZ, H4P3TZ, M4P3TZ and A4P3TZ

Conclusions

There are several known topical formulations used in treatment of autism, including the investigated compound in our study which has already been proven to be effective against this condition. However, the aim of this study was to utilize the functional groups most commonly observed in previous treatments in order to achieve a compound with improved physiochemical properties and enhanced efficiency. The procedure of substituting different functional groups in a pre-determined position of the base compound and comparison of the aforementioned properties provided us with a novel, convenient and cheap approach to reach our goal. Main purpose of the present research article is finding the novel drugs based on Zonisamide to treatment of autism disease. To attain this goal, the electronic properties, reactivity and stability

of the said compound were discussed in first step. Then, the optimized molecular structure of Zonisamide was docked into the potassium voltage-gated channel subfamily D member 2 (Kv4.2) and ligand-receptor interactions were analyzed. After that, the novel molecular structures based on Zonisamide backbone were designed and optimized. The interactions of the optimized molecular structures with the said protein were analyzed using docking study. Ten molecules showed better ligand-receptor binding than Zonisamide. Finally, the physicochemical properties of the title compounds were analyzed. Based on the molecular docking and physicochemical properties, P3TZ, H2P3TZ, M2P3TZ, H4P3TZ and M4P3TZ are our novel drugs to treatment of autism disease. We strongly believe that this method of Zonisamide-based compound screening and evaluation will be of great interest in future endeavors in drug design and drug delivery.

Conflict of interests

The authors declare that there is no conflict of interests regarding the publication of this paper.

Acknowledgments

The corresponding author is grateful to Dr. Sam Saberi Moghaddam for providing valuable suggestions.

References

- [1] C. Lord, M. Elsabbagh, G. Baird G, J. Veenstra-Vanderweele, *Lancet.*, 392, 508 (2018).
- [2] S. Goldstein, S. Ozonoff, editors. *Assessment of autism spectrum disorder*, Guilford Publications, New York (2018).
- [3] A. Masi, M.M. DeMayo, N. Glozier, A.J. Guastella, *Neurosci. Bull.*, 33, 183 (2017).
- [4] M. Varghese, N. Keshav, S. Jacot-Descombes, T. Warda, B. Wicinski, D.L. Dickstein, H. Harony-Nicolas, S. De Rubeis, E. Drapeau, J.D. Buxbaum, P.R. Hof, *Acta. Neuropathol.*, 134, 537 (2017).
- [5] D. Mandell. *Autism.*, 22, 234 (2018).

- [6] T. Hirvikoski, E. Mittendorfer-Rutz, M. Boman, H. Larsson, P. Lichtenstein, S. Bölte, *Br. J. Psychiatry.*, 208, 232 (2016).
- [7] J. Guan, G. Li, *Am. J. Public Health.*, 107, 791 (2017).
- [8] Y.I. Hwang, P. Srasuebkul, K.R. Foley, S. Arnold, J.N. Trollor, *Autism. Res.*, 12, 806 (2019).
- [9] A.M. Mosadeghrad, A. Pourreza, N. Akbarpour, *Tehran Univ. Med. J.*, 76, 665 (2019).
- [10] A.J. Baxter, T.S. Brugha, H.E. Erskine, R.W. Scheurer, T. Vos, J.G. Scott, *Psychol. Med.*, 45, 601 (2015).
- [11] S. Sandin, P. Lichtenstein, R. Kuja-Halkola, C. Hultman, H. Larsson H, A. Reichenberg A, *JAMA.*, 318, 1182 (2017).
- [12] N.S. Khanzada, M.G. Butler, A.M. Manzardo, *Int. J. Mol. Sci.*, 18, pii: E527 (2017).
- [13] J.A.S. Vorstman, J.R. Parr, D. Moreno-De-Luca, R.J.L. Anney, J.I. Jr. Nurnberger, J.F. Hallmayer, *Nat. Rev. Genet.*, 18, 362 (2017).
- [14] A. Meltzer, J. Van de Water, *Neuropsychopharmacology*, 42, 284 (2017).
- [15] I. Hertz-Picciotto, R.J. Schmidt, P. Krakowiak, *Autism. Res.*, 11, 554 (2018).
- [16] J.J. Cannell, *Rev. Endocr. Metab. Disord.*, 18, 183 (2017).
- [17] L. Guglielmi, I. Servettini, M. Caramia, L. Catacuzzeno, F. Franciolini, M.C. D'Adamo, M. Pessia, *Front. Cell. Neurosci.*, 9, 34 (2015).
- [18] C. Bagni, R.S. Zukin, *Neuron.*, 101, 1070 (2019).
- [19] R.J. Hagerman, E. Berry-Kravis, H.C. Hazlett, D.B. Jr. Bailey, H. Moine, R.F. Kooy, F. Tassone, I. Gantois, N. Sonenberg, J.L. Mandel, P.J. Hagerman, *Nat. Rev. Dis. Primers.*, 3, 17065 (2017).
- [20] S.Y. Kwan, Y.C. Chuang, C.W. Huang, T.C. Chen, S.B. Jou, A. Dash, *CNS Neurosci. Ther.*, 21, 683 (2015).
- [21] F. Brigo, S. Lattanzi, S.C. Igwe, M. Behzadifar, N.L. Bragazzi, *Cochrane Database Syst. Rev.*, 10, CD001416 (2018).
- [22] A. Reimers, H. Ljung, *Expert Opin. Pharmacother.*, 20, 909 (2019).
- [23] M. Murata, T. Odawara, K. Hasegawa, S. Iiyama, M. Nakamura, M. Tagawa, K. Kosaka, *Neurology.*, 90, e664 (2018).

- [24] K. Ikeda, M. Yanagihashi, K. Miura, Y. Ishikawa, T. Hirayama, T. Takazawa, O. Kano, K. Kawabe, N. Mizumura, Y. Iwasaki, *J. Neurol. Sci.*, 391, 5 (2018).
- [25] M. Nabati, *J. Med. Chem. Sci.*, 3, 22 (2020).
- [26] J.C. Martínez-Ávila, A. García Bartolomé, I. García, I. Dapía, H.Y. Tong, L. Díaz, P. Guerra, J. Frías, A.J. Carcás Sansuan, A.M. Borobia, *Metabolomics.*, 14, 70 (2018).
- [27] A.A. Wilfong, J.L Jr Holder, *Expert. Opin. Pharmacother.*, 12, 2573 (2011).
- [28] M. Nabati, *Chem. Methodol.*, 2, 223 (2018).
- [29] M. Nabati, *Iran. Chem. Commun.*, 7, 324 (2019).
- [30] M. Nabati, H. Sabahnoo, *J. Med. Chem. Sci.*, 2, 118 (2019).
- [31] M. Nabati, M. Kermanian, H. Mohammadnejad-Mehrabani, H.R. Kafshboran, M. Mehmannaavaz, S. Sarshar, *Chem. Methodol.*, 2, 128 (2018).
- [32] M. Nabati, *Asian J. Green Chem.*, 3, 258 (2019).
- [33] M. Nabati, *J. Phys. Theor. Chem. IAU Iran*, 14, 283 (2017).
- [34] M. Nabati, *Chem. Methodol.*, 1, 121 (2017).
- [35] M. Nabati, *J. Phys. Theor. Chem. IAU Iran*, 14, 49 (2017).
- [36] M. Nabati, M. Mahkam, Y.G. Atani, *J. Phys. Theor. Chem. IAU Iran*, 13, 35 (2016).
- [37] M. Nabati, M. Mahkam, *Org. Chem. Res.*, 2, 70 (2016).
- [38] M. Nabati, H. Sabahnoo, E. Lohrasbi, M. Mazidi, *Chem. Methodol.*, 3, 383 (2019).
- [39] D. Mandal, R. Maity, H. Beg, G. Salgado-Moran, A. Misra, *Mol. Phys.*, 116, 515 (2018).
- [40] R. Meenakshi, *J. Mol. Struct.*, 1127, 694 (2017).